PHYSICAL REVIEW C

NUCLEAR PHYSICS

THIRD SERIES, VOLUME 30, NUMBER 1 JULY 1984

Magnetic multipole excitations in ^{12}C by inelastic electron scattering

R. S. Hicks, J. B. Flanz,* R. A. Lindgren, and G. A. Peterson
University of Massachusetts, Amherst, Massachusetts 01003

L. W. Fagg
The Catholic University of America, Washington, D. C. 20064

D. J. Millener
Brookhaven National Laboratory, Upton, New York 11973
(Received 19 December 1983)

Magnetic excitations in ^{12}C have been measured by inelastic electron scattering at backward scattering angles for momentum transfers between $q=0.5$ and 3.3 fm^{-1}. Data for $M1$, $M2$, $M3$, and $M4$ transitions are compared to shell model calculations. In general, the excitation energies are reasonably predicted, as are the momentum transfer dependences of the form factors. However, the form factor magnitudes often exceed measurements by factors of more than 2. Candidates for 2^- states are seen at excitation energies of 18.2 and 22.7 MeV. It is shown how structure effects may reduce estimates of isospin mixing matrix elements from (π,π') ratios.

I. INTRODUCTION

The recent availability of large currents of spin-sensitive projectiles, made possible by a new generation of particle accelerators, has led to a vast improvement in the quality and scope of data on nuclear magnetic excitations. The understanding of these measurements has not been without difficulty. For example, a systematic deficit of strength has been identified in the (p,n) Gamow-Teller resonance,[1] and unexpectedly large $M1$ cross sections have been found in high momentum transfer (e,e').[2] Such findings have helped to stimulate theoretical conjectures regarding possible contributions from delta isobar-nucleon hole configurations,[3] possible precursor effects to meson condensation,[4] and two-pion and rho-meson exchange.[5] More orthodox explanations have also been developed, for example, core polarization.[6]

Central to many of these arguments have been the properties of magnetic excitations in ^{12}C. In large part, this interest may be attributed to the existence of the unusually strong $M1$ transition to the 15.11 MeV, $T=1$ level, which has been studied by many diverse reactions. Secondly, for ^{12}C there exist relatively sound nuclear structure models which should aid in distinguishing possible non-nucleonic processes from more conventional degrees of freedom. To help make these distinctions, a study of the multipole dependence of magnetic excitations has been advocated.[7] The nucleus ^{12}C again appears as a good choice for investigation since experimental and theoretical[8–11] studies have indicated, in addition to the strong $M1$ excitation, the existence of concentrated transition strength belonging to higher magnetic multipoles, $M2$, $M3$, and $M4$. The relatively low level density of ^{12}C should also facilitate the experimental observation of these excitations.

Despite extensive efforts, however, the spectroscopy[12] of ^{12}C magnetic transitions is still rather limited. Perhaps the only magnetic excitations with firmly-established multipolarities are those to the lowest-lying 1^+ (12.71 MeV, $T=0$ and 15.11 MeV, $T=1$) and 2^- (11.83 MeV, $T=0$ and 16.58 MeV, $T=1$) levels. Magnetic transitions to other levels are more speculative in nature. Of particular interest is a conspicuous peak observed at an excitation of 19.5 MeV in inelastic scattering experiments. However, it seems that the composition of this peak is in fact quite complex: broad and overlapped 1^-, 1^+, 2^-, 2^+, 3^-, 3^+, and 4^- states have been proposed to populate this excitation region.[12] To further complicate matters, comparisons of π^+ and π^- inelastic scattering measurements have indicated appreciable isospin mixing of some of these states with neighboring states of the same spin and parity.[13–16]

Theoretical investigations have long advocated that one of the strongest contributors to the 19.5 MeV peak is a "stretched" $M4$ transition.[10,11] Such transitions are of special interest since, in the lowest-order shell model space, the shape of the $M4$ form factor is determined solely by the $(d_{5/2},p_{3/2}^{-1})_{M4}$ matrix element, and hence cannot be influenced by configuration mixing. This restriction

has not only made such transitions "benchmarks" for the comparison of reactions involving different probes,[17] but has also permitted the separation of the different contributing transition densities.[18,19]

The higher-excitation region of ^{12}C has been studied in prior (e,e') experiments,[10,20–24] several of which lacked the resolution to separate the 19.5 MeV complex from a strongly excited 20.6 MeV peak. In light of recent concerted efforts utilizing other probes for inelastic scattering,[13–16,25–27] charge exchange,[28,29] photoproduction,[30] and radiative capture,[31–33] it seemed desirable to improve upon and perhaps reinterpret the (e,e') data. Most of the measurements reported here were carried out at backward scattering angles, where electron scattering represents one of the most selective tools available for the study of isovector magnetic transitions.[10,34]

II. THEORY

A. Shell model

For the momentum transfer region probed in this experiment, simple configuration mixing can result in $M1$, $M2$, and $M3$ form factors whose dependence is similar to that of less model-dependent $M4$ transitions. Thus, the measured magnetic form factors cannot, by themselves, be utilized to assign the spins and parities of levels. Furthermore, our low-q data are inadequate to permit the identification of low multipoles by model-independent techniques.[35] To help overcome these disadvantages and assist the interpretation of the data, we have therefore referred to the theoretical description provided by the nuclear shell model.

Shell-model calculations of magnetic excitations in ^{12}C date back more than three decades, to the work of Inglis.[36] More recently, Donnelly[10] calculated configuration-mixed 2^- and 4^- states while retaining an $s^4_{1/2}p^8_{3/2}$ ground state. The same states have been studied by Antony-Spies[11] using a 1p-1h continuum shell model. In the present work the wave functions of even-parity states were derived from the Cohen-Kurath[9] (CK) (8–16)2BME two-body matrix elements. The odd-parity states have been calculated in a $1\hbar\omega$ space with the Millener-Kurath[37] (MK) effective interaction. A comparison of the observed and calculated level spectra is shown in Fig. 1.

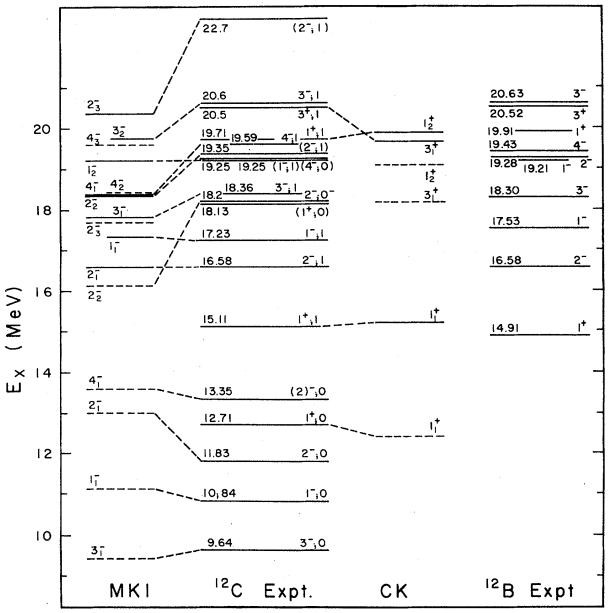

FIG. 1. Partial energy level schemes of ^{12}C and its analog, ^{12}B. In the theoretical spectrum, calculated using the Millener-Kurath (Ref. 37) and Cohen-Kurath (Ref. 9) interactions, dashed levels have $T=0$. The remaining theoretical levels are $T=1$ states. The calculated energy levels are fixed to the ^{12}C ground state and the 2^- level at 16.58 MeV. For the sake of clarity, 0^-, 0^+, 2^+, and 4^+ levels have been omitted.

Apart from the transitions to the lowest-lying $T=0$ and $T=1$ 1^+ states, the best experimental candidate for a magnetically excited, even-parity state is a proposed $T=1$, 3^+ level at 20.5 MeV. The majority of the transverse strength above 15 MeV appears to arise from magnetic excitation of odd-parity levels. As indicated in Table I, the wave functions of these states can be expressed in terms of an sd-shell particle, usually $s_{1/2}$ or $d_{5/2}$, coupled to the odd-parity states of an $A=11$ core. In ^{11}B the important levels are the $\frac{3}{2}^-$ ground state and excited states at 2.12 MeV ($\frac{1}{2}^-$), 4.45 MeV ($\frac{5}{2}^-$), 5.02

TABLE I. Weak-coupling decompositions of $T=1$ odd-parity wave functions.

J_n	E_x[a] (MeV)	Wave function
2_1	16.58	$-0.44\frac{3}{2}_1\times d_{5/2}+0.83\frac{3}{2}_1\times s_{1/2}+0.23\frac{5}{2}_1\times d_{5/2}$
1_1	17.23	$0.23\frac{3}{2}_1\times d_{5/2}+0.87\frac{3}{2}_1\times s_{1/2}$
3_1	18.36	$-0.92\frac{3}{2}_1\times d_{5/2}+0.21\frac{5}{2}_1\times s_{1/2}$
1_2	19.25	$0.88\frac{1}{2}_1\times s_{1/2}+0.21\frac{5}{2}_1\times d_{5/2}+0.31\frac{3}{2}_2\times d_{5/2}$
2_2	19.35	$-0.68\frac{3}{2}_1\times d_{5/2}-0.40\frac{3}{2}_1\times s_{1/2}+0.49\frac{1}{2}_1\times d_{5/2}$
4_1	19.59	$0.90\frac{3}{2}_1\times d_{5/2}-0.29\frac{5}{2}_1\times d_{5/2}$
3_2	20.6	$0.84\frac{1}{2}_1\times d_{5/2}-0.21\frac{5}{2}_1\times d_{5/2}-0.22\frac{3}{2}_2\times d_{5/2}+0.33\frac{5}{2}_1\times s_{1/2}$
2_3	22.7	$-0.57\frac{1}{2}_1\times d_{5/2}-0.63\frac{3}{2}_2\times d_{5/2}+0.28\frac{1}{2}_1\times d_{3/2}$

[a]Energy of observed level with which the shell-model state is identified.

MeV ($\frac{3}{2}^-$), and 6.75 MeV ($\frac{7}{2}^-$). The $T=1$ wave functions consist of only a few components, but the $T=0$ wave functions are considerably more complex. This feature can be understood in terms of the supermultiplet classification scheme. The $A=11$ wave functions have a simple LS structure based on the p^7 [43] configuration which accounts for 82% to 95% of the relevant core wave functions. Coupling an sd-shell particle to p^7 [43] leads to [44] ($TS=00$) or [431] ($TS=01,10,11$) symmetries for $A=12$ odd-parity states. The [44] symmetry is strongly favored by the effective interaction so that the lowest $T=0$ wave functions have a dominant $L=J$, $S=0$ structure as can be seen from Table II. The intensity of the [44] symmetry is slightly less than the fraction of $S=0$, and is about the same as the [44] component in the ^{12}C ground state. In addition, the intensity of the SU(3) configuration (33) from $p^7(13)\times sd(20)$ is high for almost all the states listed in Table II. The spectrum of low-lying $T=0$ states is naturally similar to that obtained from three α-cluster models. In terms of the weak-coupling basis, the more complex nature of the $T=0$ wave functions arises because a weak-coupling basis state, in general, contains both $S=0$ and $S=1$ components, and hence an admixture of various basis states is required to purge the $S=1$ components. For $T=1$ both $S=0$ and $S=1$ occur in the same supermultiplet and no similar requirement exists.

Figure 1 shows some deficiencies in the ability of the $1\hbar\omega$ calculation to reproduce the experimental level spectrum in the region 16—21 MeV. This can be traced mainly to the tendency for levels of basically $s_{1/2}$ character, the 2_1^-, 1_1^-, and 1_2^- $T=1$ states, to come too high relative to the remaining states which are primarily of $d_{5/2}$ character. It is probable that the spectrum could be much improved by relatively minor adjustments to the MK interaction. Such modifications should not greatly change the wave functions, since only the mixing of the 4_2^- and 4_3^- $T=0$ states, just 1.1 MeV apart, appears sensitive to small changes in the interaction. Some of the arguments for the identifications made in Fig. 1 are presented in Sec. IV. As shown in Fig. 1, many of the $T=1$, unnatural-parity levels have known analogs in ^{12}B. In the case of ^{12}C 19.5 MeV complex, the existence of 4^-, 2^-, and 1^- analog levels in the corresponding excitation region of ^{12}B provides an invaluable lead for the interpretation of the data presented here.

The magnetic form factors have been calculated using the one-body density matrix elements listed in Table III, with corrections[10] applied for nucleon finite size and the lack of translational invariance of the shell model wave functions. For the most part, the form factors have been determined using harmonic oscillator radial wave functions with an oscillator parameter of $b=1.65$ fm. Although this value is reasonably consistent with ground-state properties,[10] it may, by no means, be rigidly fixed since it is unrealistic to restrict all single-particle orbits to the same bound harmonic oscillator potential well. In addition, calculations were performed with wave functions derived from a Woods-Saxon potential well of diffuseness 0.5 fm and radius $1.25(A-1)^{1/3}$ fm. The spin-orbit splitting was set to 6 MeV for both the $1p$ and $1d$ orbitals, and the single-particle energies were $E(1s_{1/2})=-38$ MeV, $E(1p_{3/2})=-16$ MeV, $E(1p_{1/2})=-10$ MeV, $E(1d_{5/2})=E(2s_{1/2})=E(1d_{3/2})=-2$ MeV. For the range of momentum transfer explored in this experiment, the shapes of the form factors obtained with Woods-Saxon radial wave functions were very similar to the results of the harmonic oscillator calculations. However, the relative magnitudes of the Woods-Saxon and harmonic oscillator form factors varied from transition to transition. The largest difference occurred for $M2$ transitions with a large $(2s_{1/2},1p_{3/2}^{-1})$ matrix element, where the Woods-Saxon calculations were found to lie about 20—25% below the harmonic oscillator form factors.

In general, the calculated form factors are very similar to those given in previous theoretical studies. However, in

TABLE II. LS structure of ^{12}C odd-parity states.

J_n	T	E_x[a] (MeV)	Intensity (%) $L,S=J,0$	$J-1,1$	$J,1$	$J+1,1$	$(3,3)$[b]
3_1	0	9.64	88.0	5.5	2.8	3.1	91.0
1_1	0	10.84	85.5	3.1	3.2	7.3	76.3
2_1	0	11.83	72.1	16.7	6.4	2.4	81.7
4_1	0	13.35	81.8	12.7	2.9	1.5	90.4
2_2	0	18.2	44.6	35.5	7.9	8.3	7.7
4_2	0	19.25	29.2	52.7	8.6	1.1	67.6
4_3	0	(20.7)	50.2	41.7	4.0	0.6	82.4
2_1	1	16.58	11.6	63.3	17.1	3.2	68.2
1_1	1	17.23	31.9	3.3	33.6	27.6	55.4
3_1	1	18.36	17.9	56.5	19.0	3.5	65.4
1_2	1	19.25	34.7	0.9	52.6	10.8	74.6
2_2	1	19.35	9.2	62.0	19.1	6.4	21.6
4_1	1	19.59	8.7	72.3	13.5	1.0	69.7
3_2	1	20.6	13.8	33.4	48.2	3.0	85.2
2_3	1	22.7	21.0	18.6	4.7	52.5	74.6

[a]Energy of observed level with which the shell-model state is identified.
[b]Intensity of the dominant SU(3) representation.

TABLE III. One-body density matrix elements[a] for ^{12}C odd-parity transitions.

J_n	T	E_x[b] (MeV)	$2s_{1/2}p_{1/2}$	$d_{3/2}p_{1/2}$	$d_{5/2}p_{1/2}$	$2s_{1/2}p_{3/2}$	$d_{3/2}p_{3/2}$	$d_{5/2}p_{3/2}$	$p_{1/2}1s_{1/2}$	$p_{3/2}1s_{1/2}$
3_1	0	9.64			0.2645		−0.3145	0.5099		
1_1	0	10.84	0.2701	0.0999		0.6306	−0.1219	0.3195	0.0543	−0.0436
2_1	0	11.83		−0.710	−0.1216	−0.3956	0.1639	−0.3875		−0.0199
4_1	0	13.35						0.3390		
2_2	0	18.2		−0.0144	0.0924	0.2783	0.1189	−0.6988		0.0107
4_2	0	19.25						−0.6531		
4_3	0	(20.7)						0.3609		
2_1	1	16.58		−0.0332	0.0047	0.7079	−0.0050	0.3474		0.0133
1_1	1	17.23	0.1073	0.0031		−0.7172	0.1199	−0.1773	−0.0842	0.0235
3_1	1	18.36			−0.0384		−0.1322	−0.7510		
1_2	1	19.25	−0.5280	0.0021		−0.0947	−0.0150	−0.0652	−0.0283	−0.0216
2_2	1	19.35		−0.0678	−0.2973	−0.3213	−0.0904	0.5521		−0.0074
4_1	1	19.59						−0.8069		
3_2	1	20.6			0.5027		0.1497	−0.0613		
2_3	1	22.7		−0.1670	0.3429	−0.1096	−0.4802	0.1957		−0.0063

[a]The definition of the one-body matrix element, together with the single-particle phase conventions are given in Ref. 38. For ^{12}C these one-body matrix elements are equal to the transition amplitudes Z_T defined in Ref. 58.
[b]Energy of observed level with which the shell-model state is identified.

some cases there exist notable differences in the magnitudes of the expected form factors. For example, Donnelly[10] finds that the full isovector $M4$ strength is concentrated in a state that he predicts at 20.17 MeV. In our calculations, the corresponding state carries only 65% of the full single-particle strength.

As noted by Donnelly,[10] transverse electron scattering is primarily sensitive to isovector $\Delta T=1$ transitions since the isovector magnetic moment $\mu_v=(\mu_n-\mu_p)/2=-2.353$ μ_N is large compared to the isoscalar magnetic moment $\mu_s=(\mu_n+\mu_p)/2=0.440$ μ_N. The large value of μ_v also accounts for the expected dominance of spin-flip terms in the measured isovector form factors. However, for the case of isoscalar $\Delta T=0$ transitions, purely convective currents can contribute much more equitably. For example, the calculations indicate that the first $\Delta T=0$, $M2$ form factor is dominated by spin-independent convection current terms, and that the first diffraction maximum of the 12.71 MeV isoscalar $M1$ transition is greatly reduced by destructive interference between spin-flip and convection current contributions. The LS-coupling model also contributes to the understanding of these effects. As can be observed from Table II, whereas the lowest $T=0$ states are mainly $S=0$ in character, $S=1$ components predominate in the $T=1$ wave functions.

B. Isospin mixing

Differences between measured π^+ and π^- inelastic scattering cross sections identify[13–16] three pairs of isospin-mixed levels in ^{12}C: the lowest-lying 1^+ states at 12.71 and 15.11 MeV, a pair of tentative 2^- levels at 18.32 and 19.35 MeV, and a probable 4^- doublet at 19.25 and 19.65 MeV. Under specific model assumptions, namely that the pure isospin states being mixed have the same particle-hole structure and spatial distribution, charge-dependent isospin-mixing matrix elements have been calculated from observed ratios of π^+ and π^- cross sections.[13,14] In the following, a simple two-state mixing formalism is developed which allows for the evaluation of isospin mixing without the imposition of restrictive model assumptions.

For magnetic transitions in a $J=0^+$, $T=0$ nucleus, the plane-wave cross section for inelastic electron or pion scattering to a state of good isospin $T=0$ or $T=1$ can be written

$$\sigma_T^{1/2}(q)\sim G_T^l P_T^l(q)+G_T^s P_T^s(q)\ ,$$

where $P_T^l(q)$ and $P_T^s(q)$ are the momentum representations of the orbital and spin transition densities. Applied to electron scattering, the orbital and spin g factors $G_0^l=G_1^l=\frac{1}{2}$, and $G_0^s=\mu_s$, $G_1^s=\mu_v$. For (π,π'), $G_0^l=G_1^l=0$, and G_0^s and G_1^s are the Fourier transforms of the isoscalar and isovector components of the pion-nucleon spin-orbit potential. In the latter case, it is convenient to omit the spin superscript s and replace it with a $+$ or $-$ sign to indicate π^+ or π^- scattering. Near the $N^*(3,3)$ resonance, $G_0^+/G_1^+=-2$, $G_0^-/G_1^-=2$, and $G_1^+/G_1^-=-1$. For a pair of isospin-mixed states $|A\rangle$ and $|B\rangle$,

$$\sigma_A^{1/2}(q)\sim-\beta\sigma_1^{1/2}+(1-\beta^2)^{1/2}\sigma_0^{1/2}$$

and

$$\sigma_B^{1/2}(q)\sim\beta\sigma_0^{1/2}+(1-\beta^2)^{1/2}\sigma_1^{1/2}\ ,$$

where β is the mixing parameter. Since the absolute (π,π') cross sections are less well understood then the electromagnetic results, the analysis of the pion data is usually based on cross section ratios, for example,

$$[\sigma_A^+(q)/\sigma_A^-(q)]^{1/2}=[2x+S(q)]/[2x-S(q)]\ ,$$

$$[\sigma_B^+(q)/\sigma_B^-(q)]^{1/2}=[xS(q)-2]/[xS(q)+2]\ ,$$

and

$$[\sigma_A^+(q)/\sigma_B^+(q)]^{1/2}=[2x+S(q)]/[2-xS(q)]\ ,$$

where $x=(1-\beta^2)^{1/2}/\beta$, and $S(q)=P_1^s(q)/P_0^s(q)$. Differences between π^+ and π^- distortion effects modify these ratios by only a few percent.[39] In principle, therefore, by solving for any two (π,π') cross section ratios one can determine not only the isospin mixing parameter β, but also the density ratio $S(q)$, albeit with a sign ambiguity. Note that, in contrast with previous analyses which set $S(q)=1$, corresponding to $P_1^s(q)=P_0^s(q)$, no explicit structure assumptions have been imposed in the present formalism.

In practice, the (π,π') cross section ratios are not usually determined with sufficient precision to accurately define β and $S(q)$. Additional information from the absolute (π,π') and (e,e') cross sections is helpful, not only to further restrict β and $S(q)$, but also to give the absolute densities $P_0^s(q)$ and $P_1^s(q)$. For example, whereas the total (e,e') cross section for states $|A\rangle$ and $|B\rangle$ is dominantly isovector in character, the summed (π,π') cross section is primarily sensitive to the isoscalar spin-flip density, according to

$$\sigma_A^{\pm}+\sigma_B^{\pm}=\sigma_0^{\pm}+\sigma_1^{\pm}$$
$$\sim G_0^{\pm 2}[P_0^{s^2}(q)+P_1^{s^2}(q)/4]\ ,$$
$$\sim[G_0^{\pm}P_0^s(q)]^2[1+S^2(q)/4]\ .$$

An analysis following these ideas will be developed in Sec. IV C.

III. EXPERIMENTAL METHOD AND DATA ANALYSIS

The measurements were performed using the high-resolution electron scattering facility[40] of the Bates Linear Accelerator Laboratory in Middleton, Massachusetts. Most of the data were obtained through the use of a 180° scattering apparatus;[41] however, we have also utilized calibration measurements from experiments performed at 90°, 140°, and 160°. Incident beam energies of 50.7–338.0 MeV were employed, with a corresponding range of 0.51–3.28 fm^{-1} in the elastic momentum transfer. The targets consisted of natural carbon foils with effective thicknesses varying from 25.9 to 139.6 mg cm^{-2}. Although the thinnest targets gave momentum resolutions as fine as 80 keV/c, thicker targets were often chosen to improve the counting statistics.

The correct normalization of the 90° form factors was established using the known ^{12}C elastic cross section.[42] At more backward scattering angles, the ^{12}C data were normalized by comparing measured proton elastic cross sections with the known values.[43] The largest spectrometer aperture subtended 26.8×130.9 mrad at the target, corresponding to an acceptance solid angle of 3.51 msr. Inelastic cross sections were determined using a line-shape fitting procedure and converted into (e,e') form factors.[44] First-order Coulomb distortion corrections were made by transforming the data to effective momentum transfers, defined by[45]

$$q_{\rm eff}=q[1+f(q)Z\alpha/ER]\ ,$$

where E is the incident electron energy and $R=3.16$ fm is the radius of the equivalent nuclear sphere. For the measured kinematic range in ^{12}C, the function $q_{\rm eff}$ can be approximated by $f(q)=0.3+0.5q$, where q is in units of fm^{-1}. This dependence was established by comparing plane-wave Born approximation $M4$ form factors with those calculated in the distorted wave Born approximation. Complete tables of the data have been deposited with the Physics Auxiliary Publication Service.[46]

IV. RESULTS

Two scattered electron spectra are shown in Fig. 2. The arrows denote the known and probable magnetic transitions, now to be discussed.

A. The known 1^+ states

Although the $M1$ form factors for the excitation of the 1^+ states at 12.71 ($T=0$) and 15.11 MeV ($T=1$) have been presented elsewhere,[47] it is useful to review the pertinent facts. The $B(M1)\uparrow=2.47\ \mu_N^2$ given by the CK wave functions for the 15.11 MeV transition is 13% smaller than the observed value of 2.79 μ_N^2. However, with the inclusion of one-pion exchange currents,[48] the theoretical prediction is raised to 2.78 μ_N, and essentially exact agreement is obtained. Extensive study[49] has been directed to higher momentum transfers, where (e,e') data on the second diffraction maximum of the $M1$ form factor exceed the CK prediction by about a factor of 10. This discrepancy has been attributed to various effects, e.g., core polarization,[6] or mesonic interactions of shorter range than one-pion exchange.[4,5] More simply, Dubach and Haxton[50] demonstrated how a relatively small readjustment of the CK shell model amplitudes is sufficient to account for much of the high-q discrepancy. The CK

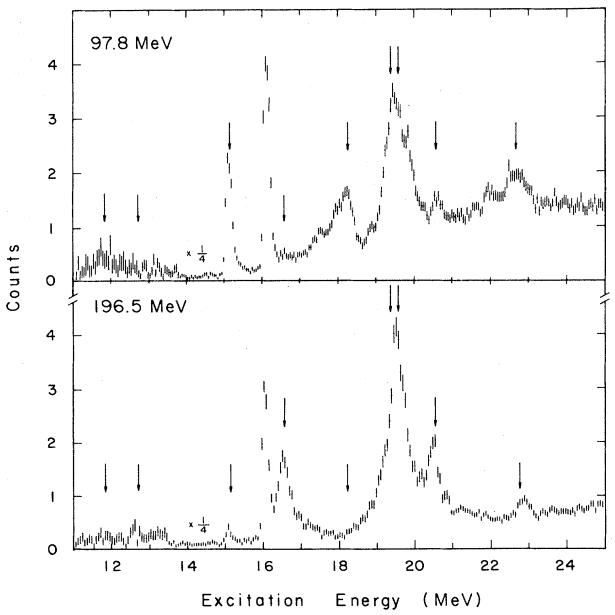

FIG. 2. Two examples of (e,e') spectra measured at 180°. The arrows denote known and probable magnetic transitions discussed in the text.

predictions underestimate the first diffraction maximum of the isoscalar 12.71 MeV form factor by a factor of 3. However, Flanz *et al.*[47] have shown that the form factor is sensitive to isospin mixing with the 15.11 MeV $T=1$ level. The amount of mixing required to give agreement with the data corresponds to a charge-dependent isospin-mixing matrix element of 140±35 keV. This is in good agreement with the 148±29 keV recently derived by Morris *et al.*[15] from inelastic pion scattering measurements. The ratio of the (π,π') cross sections for the 15.11 and 12.71 MeV transitions varies with incident pion energy and, in particular, exceeds the expected four-to-one ratio at energies near the $N^*(3,3)$ resonance. Morris *et al.*[51] have suggested that this behavior may reflect the excitation of delta particle-nucleon hole configurations in the $T=1$ wave function. An earlier proposal,[4,52] based on the large 15.11 MeV cross sections observed in high-q (e,e'), that ^{12}C might be close to the pion-condensation threshold, appears to be inconsistent with the results of more recent inelastic proton scattering experiments.[27,53]

B. The 11.83 and 16.58 MeV 2^- states

In Fig. 3 the form factors for the transitions to the 2^- states at 11.83 ($T=0$) and 16.58 MeV ($T=1$) are compared to the harmonic oscillator shell model predictions. In both cases the observed q dependence is consistent with the theory, however, a notable aspect is the extent to which the shell model calculations overestimate the data on the 11.83 MeV transition. Although the predicted

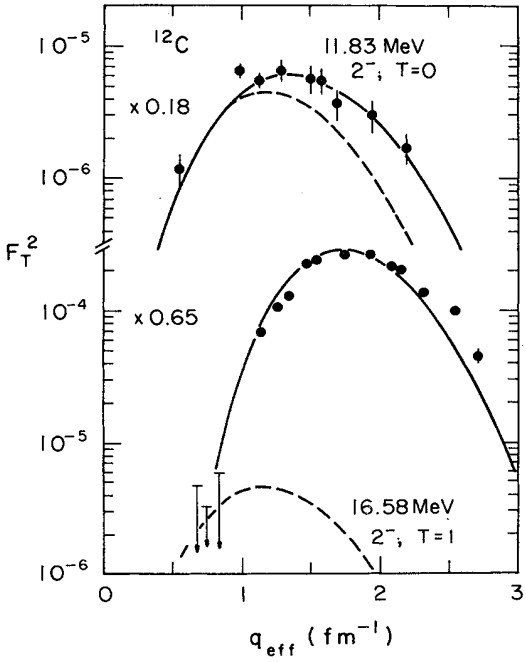

FIG. 3. Comparison of measured and calculated form factors for the 11.83 and 16.58 MeV $M2$ transitions. The theoretical curves were computed using harmonic oscillator radial wave functions with $b=1.65$ fm, and have been reduced by the indicated factors. The continuous curves represent the total calculated form factors, whereas the dashed curves exclude spin-flip contributions.

16.58 MeV form factor is just 35% too large, the 11.83 MeV calculation must be reduced by a factor of 5.5 in order to agree with the data. A recomputation of the 11.83 MeV form factor using Woods-Saxon radial wave functions leaves the theoretical predictions essentially unchanged, and consequently does not alleviate the disagreement. [Compared to the 11.83 MeV excitation, the 16.58 MeV transition has a more dominant $(2s_{1/2},1p_{3/2}^{-1})$ character and the form factor is sensitive to the form of the radial wave functions. The Woods-Saxon form factor for the 16.58 MeV transition exceeds the data by only 15%.] Furthermore, it appears unlikely that the small 11.83 MeV form factor can be attributed to isospin mixing with the 16.58 MeV, $T=1$ state, since this would not only demand an unreasonably large charge-dependent mixing matrix element, but would also destroy the good theoretical description of the 11.83 MeV form factor shape. Indeed, it is remarkable that the $\Delta T=0$ shell model calculation can be so far awry in magnitude and yet correctly describe the shape of the low-multipole form factor, which is sensitive to the configuration admixture in the initial and final state wave functions.

Figure 4 shows that the strongest isoscalar $M2$ transition is predicted to excite the second $T=0$, 2^- state, calculated to lie at 16.14 MeV. One might seek to identify this state with a 375±40 keV wide, $T=0$ unnatural-parity state observed at 13.35 MeV and tentatively assigned[12] as $J=2^-$, although the evidence for such an assignment is very weak. Such an identification seems to be inconsistent with the present measurements which show no contribution from the 13.35 MeV peak. Near $q=1$ fm^{-1}, where the theoretical form factor reaches a maximum value of 1.2×10^{-4}, the data set an upper limit of 4×10^{-6} on the 13.35 MeV form factor. The level of this discrepancy makes it unlikely that the 13.35 MeV level could correspond to the second calculated $T=0$, 2^- state. As will be seen, the next good candidate for a (dominantly) isoscalar $M2$ excitation appears to have been found in the vicinity of 18.2 MeV.

If the 13.35 MeV level is not 2^-, as suggested by the present results, can it be identified with the first predicted $T=0$, 4^- state, calculated at 13.59 MeV? The calculated

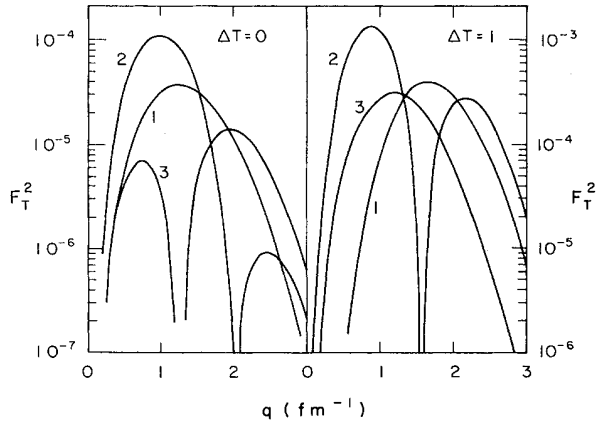

FIG. 4. Harmonic oscillator form factors calculated for the three lowest-energy $\Delta T=0$ and $\Delta T=1$ $M2$ excitations.

$M4$ form factor peaks near $q=1.75$ fm^{-1}, reaching a magnitude of 1.1×10^{-5}. This exceeds by a factor of 7 the upper limit set by the data in this momentum transfer region.

C. The 4$^-$ states

The form factor deduced for the 19.5 MeV complex is shown in Fig. 5(a). The dominantly transverse nature of this peak is proven by the near equivalence of the 90° and 180° data. In the momentum transfer range $q=1$–2.5 fm^{-1}, an upper limit of $|F_L|^2\leq10^{-4}$ may be set on the corresponding longitudinal form factor. The data have been combined with the low-q measurements of Goldemberg and Barber.[20] Results obtained by Lightbody[23] and Beer *et al.*[21] lie in general agreement with the data shown in Fig. 5(a), but have somewhat larger errors. Although measurements made at Stanford[10] extend to $q=3.67$ fm^{-1}, the 19.5 and 20.6 MeV peaks were not satisfactorily resolved. The experiment of Yamaguchi *et al.*,[24] which barely resolved these peaks, gave form factors consistent with the present results, except in the $q=1.5$–2 fm^{-1} region, where the data of Yamaguchi *et al.* are 20% lower.

Figure 5(a) shows a steep low-q rise in the form factor followed by a more gradual dependence at higher momentum transfers. This lack of a simple diffraction structure points to the presence of two or more contributing multipoles. As mentioned earlier, in the corresponding excitation region of the analog nucleus ^{12}B, 4$^-$, 2$^-$, and 1$^-$ levels have been identified.[12] Moreover, various theoretical studies[10,11] insist upon the existence of a very strong $\Delta T=1$, $M4$ excitation in this region. In the present calculations, the energy of this excitation is 18.35 MeV. The q dependence of the stretched $M4$ transition strength is such that it may be expected to dominate the data taken at high momentum transfers.

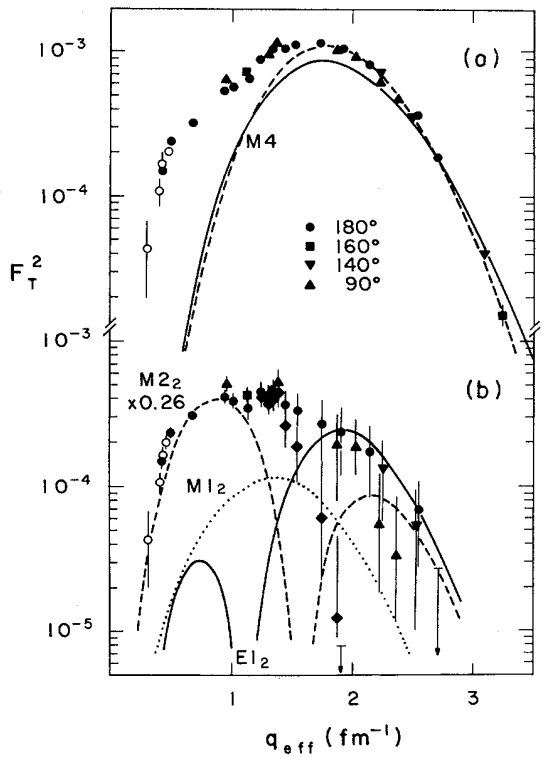

FIG. 5. (a) Form factor data for the 19.5 MeV complex. The curves show the presumed $M4$ contributions. The continuous curve has the same q dependence as that observed for $M4$ transitions in ^{13}C. The dashed curve represents a harmonic oscillator $M4$ fit to the ^{12}C data alone. (b) Residual form factor remaining after the subtraction of the $M4$ component. The diamonds were derived under the assumption that the $M4$ form factor is represented by the dashed curve in (a). Other data points were obtained by subtracting the continuous curve. Comparisons are made with three calculated shell-model transitions.

Our procedure for analyzing the 19.5 MeV complex is as follows. Except for the adjacent 20.6 MeV peak, the cross section of which has been determined by a separate line shape fitting procedure, it is assumed that the highest-q data define only the isovector $M4$ cross section. Assuming further that the $M4$ cross section extrapolates to lower momentum transfers in accordance with model descriptions, it is then possible to subtract out the $M4$ component and study explicitly the properties of the residual cross section.

A critical element in this analysis is the selection of an appropriate q dependence for the $M4$ form factor. Fortunately, because of the strong dominance of the $(d_{5/2},p_{3/2}^{-1})_{M4}$ matrix element, the $M4$ form factor shape is expected to be largely independent of configuration mixing effects. Perhaps the soundest assumption that can be made is that the ^{12}C form factor has the same q dependence as that measured[54] for $M4$ transitions in ^{13}C. Although the $M4$ form factor shape is directly influenced by radial potential-well parameters, the observed equivalence of the ^{12}C and ^{13}C root-mean-square charge radii[55] suggests, for protons at least, that any well-size differences should be minimal. Furthermore, possible concern that continuum effects might make the form factor shape dependent upon excitation energy seems unwarranted: In ^{13}C, where measurements have been made of three $M4$ transitions distributed over a 12 MeV excitation range, no such dependence has been seen.[54,56]

The results of this analysis are shown in Figs. 5 and 6. The solid curve in Fig. 5(a) follows the shape of the ^{13}C $M4$ form factor. This is seen to provide a good description of the ^{12}C 19.5 MeV data above about $q=2$ fm^{-1}. Selected experimental spectra are shown on the left-hand side of Fig. 6 with the continuous curves delineating the separate contributions of the 20.6 MeV resonance, assumed $M4$ line shape, and underlying continuum. The latter curve was determined empirically by fitting to an extended range of scattered electron energies. As defined by the highest-q data, the $M4$ cross section peaks at 19.59 ± 0.04 MeV, and has a half-maximum full-width of 0.55 ± 0.07 MeV. Inelastic pion scattering measurements at high momentum transfer show a pair of states in this excitation region,[13] one at 19.25 ± 0.05 MeV, and the other at 19.65 ± 0.05 MeV. By virtue of marked asymmetries observed in the relative π^+ and π^- cross sections, this pair of states has been interpreted as an isospin-mixed doublet. The present analysis does not easily permit any statement regarding the number of 4$^-$ states in the 19.5 MeV region. It can only be assumed that the high-q (e,e′)

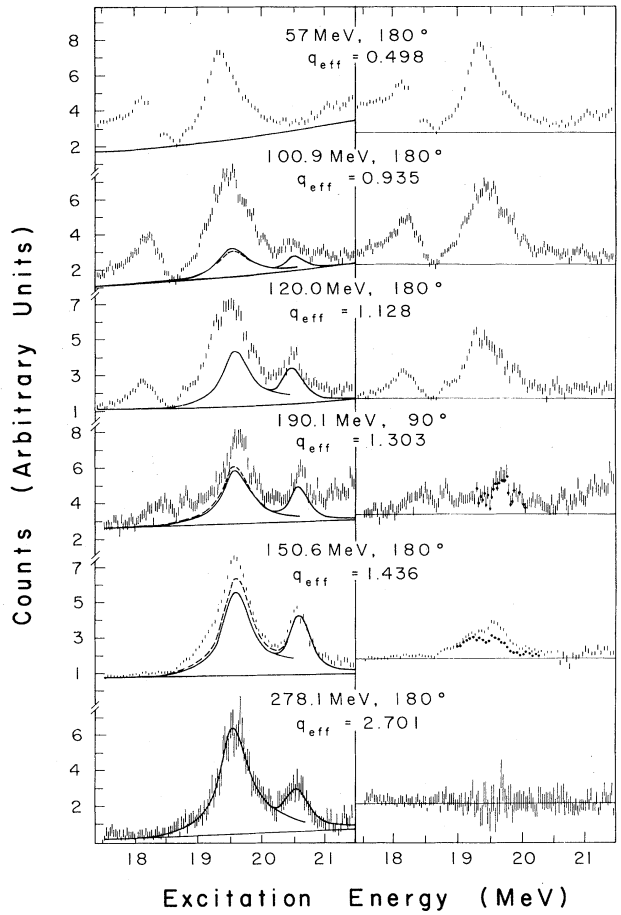

FIG. 6. Shown on the left-hand side are selected experimental spectra for data in the region of the 19.5 MeV complex. The curves delineate the separate contributions of the 20.6 MeV resonance, assumed $M4$ line shape, and underlying continuum. Two possible choices, represented by continuous and dashed curves, are given for the $M4$ differential cross section. These correspond to the continuous and dashed curves depicted in Fig. 5(a). On the right-hand side of the figure are residual cross sections remaining after the subtraction of the continuum, $M4$, and 20.6 MeV contributions. The plain error bars are based on the assumption that the $M4$ cross section follows the continuous curves. The circles employ the dashed curves.

cross sections reflect the distribution of isovector $M4$ strength.

For a nucleus with a ground state spin of zero, a common measure of the stretched magnetic transition strength is in terms of that expected for the leading-order component in the extreme-single-particle model.[17] In the plane-wave Born approximation, and with harmonic oscillator radial wave functions, the $M4$ form factor for the relevant $(d_{5/2},p_{3/2}^{-1})_{M4,\Delta T=1}$ matrix element is given by[57]

$$|F_{M4}(q)|^2=0.031(\text{fm}^2)y^4 f_{\text{cm}}^2 f_{\text{sn}}^2 e^{-2y}b^{-2}\ , \qquad (1)$$

where $y=(bq/2)^2$, and f_{cm}^2 and f_{sn}^2 are the center-of-mass and nucleon finite size terms. The value of the oscillator parameter which best fits the ^{13}C data in the vicinity of the form factor peak is $b=1.53$ fm. With this value, the $M4$ strength in the ^{12}C 19.5 MeV complex was found to equal $34\pm4\%$ of the isovector extreme single-particle limit given by Eq. (1). According to recent calculations by Plum *et al.*,[19] the consideration of one-pion exchange currents reduces the deduced strength by about 15%; however, this correction is approximately offset by the effect of employing more realistic Woods-Saxon wave functions in the analysis.[56]

In order to assess the model dependence of the above analysis, alternative interpretations were explored. One, for example, did not rely upon the form factor shape measured for ^{13}C, but instead was based on directly fitting the ^{12}C high-q data with the harmonic oscillator, $M4$ form factor given by Eq. (1). In this case there were two free parameters, an overall $M4$ strength factor, and the oscillator parameter b. The data above $q=1.7$ fm^{-1} are best fit with $b=1.52\pm0.01$ fm^{-1} and an $M4$ strength equal to $40\pm4\%$ of the isovector single-particle limit. This fit is represented in Figs. 5(a) and 6 by the dashed curves.

Neither of the above analyses gives any consideration to high-q contributions from multipoles other than $M4$. According to theoretical results to be discussed in Sec. IV D, the strongest non-$M4$ contribution is expected to come from an $E1$ excitation to the analog of the 4.30 MeV, 1^- state in ^{12}B. If this transition indeed carries the full strength predicted by the shell model, the deduced $M4$ strengths will be reduced by not more than 20%.

For the 19.25 MeV peak observed in (π,π'), the cross section ratio σ_A^+/σ_A^- has been judged by Morris *et al.*[13] to be greater than 2. Under the assumptions of two-state mixing and $S(q)=1$, they found a rather large lower bound of 0.32 for the mixing parameter β. The utilization of the estimated cross section ratio[13] $\sigma_B^+/\sigma_B^-<\frac{1}{2}$ for the second, 19.65 MeV peak permits the relaxation of the assumption that $P_0^s(q)=P_1^s(q)$. Solutions obtained in this more general analysis extend throughout the hatched area in the plot of the density ratio $S(q)$ against β shown in Fig. 7. Note that the (π,π') cross sections do not uniquely define the signs of $S(q)$ and β: An identical solution area exists in the quadrant where both $S(q)$ and β are negative. With the possible exception of σ_A^+/σ_B^-, other (π,π') cross section ratios do not provide any significant further confinement of the solution region. Although neither $S(q)$ nor β are well determined by the more general analysis, an absolute lower limit of 0.17 may be imposed on $|\beta|$, about half the limit deduced by Morris *et al.* under the assumption $S(q)=1$. Even if it was argued, on theoretical grounds, that $S(q)$ should be close to unity, Fig. 7 shows that in the vicinity of $S(q)=1$, the lower limit that may be imposed on $|\beta|$ varies rapidly.

To better constrain the lower bound on the isospin mixing, a separate determination of $S(q)$ would clearly be helpful. This may be provided by the absolute (e,e') and (π,π') cross sections, summed over states $|A\rangle$ and $|B\rangle$. For this interpretation it is convenient to attribute the one-body $M4$ transition density solely to the stretched $(d_{5/2},p_{3/2}^{-1})_{M4}$ single-particle density $\rho_T^s(q)$, writing

$$P_T^s(q)=Z_T\rho_T^s(q)\ ,$$

where the transition amplitudes Z_T take on the value of unity for a pure particle-hole excitation.[58] In particular,

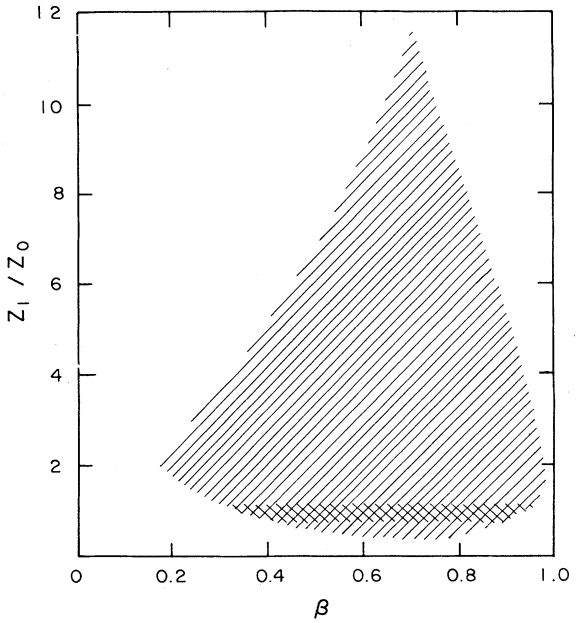

FIG. 7. Solution regions for isospin mixing between 4^- states in ^{12}C. The axes are the isospin mixing parameter β and the ratio of the isovector and isoscalar spin transition densities S. The singly hatched area represents the allowed solution region when only (π,π') cross section ratios are considered. If the absolute (π,π') and (e,e') cross sections are adopted as additional constraints, the solution region is confined to the doubly hatched area.

this assumption simplifies the interpretation of the (e,e') cross sections since the corresponding orbital transition densities $\rho_0^l(q)$ and $\rho_1^l(q)$ vanish for the stretched matrix element. Possible shape differences between the isoscalar and isovector densities are neglected, and we set $\rho_0^s(q)=\rho_1^s(q)$. Considering the model uncertainty in the extraction of the $M4$ strength, the above analysis of the (e,e') data gives

$$(\sigma_A+\sigma_B)/\sigma_1=Z_1^2+0.035Z_0^2 =0.34\pm0.07\ , \quad (2)$$

where σ_1 represents the pure single-particle isovector cross section.

A similar relationship can be derived by comparing the $(\pi^+,\pi^{+\prime})$ cross sections measured by Moore *et al.*[25] with the distorted-wave, continuum shell model calculations of Halderson *et al.*[59] Recently, (e,e') and (p,p') results have been employed[39,56] to test the accuracy of the distorted-wave (π,π') calculations for $M4$ transitions in ^{16}O and ^{13}C. Although it was found necessary to increase the predicted ^{16}O(π,π') cross sections by about 30%, data on the 9.5 MeV $M4$ transition in ^{13}C showed little need for such a large renormalization. The 162 MeV $(\pi^+,\pi^{+\prime})$ cross sections measured by Moore *et al.*[25] account for about 37% of the total predicted particle-hole strength,[59] i.e.,

$$(\sigma_A^+ +\sigma_B^+)/(\sigma_0^+ +\sigma_1^+)=0.8Z_0^2+0.2Z_1^2 =0.37\ . \quad (3)$$

It can be assumed that the error in this result is no better than that in the (e,e') analysis. Together, Eqs. (2) and (3) give $|Z_0|=0.62\pm0.10$, $|Z_1|=0.57\pm0.07$, and $|S|=0.9\pm0.2$. The last result, which is consistent with the assumption made by Morris *et al.*, sets for $|\beta|$ a three standard-deviation lower limit of about 0.22. This value corresponds to a lower limit of 86 keV for the charge-dependent isospin mixing matrix element, rather than the 120 keV obtained by Morris *et al.*[13] As noted by Halderson *et al.*,[59] appreciable mixing between the two levels is not unexpected. Large Coulomb mixing matrix elements result not only from the similarity of the unperturbed wave functions, but also from the unbound nature of the states.

In comparison with the shell-model prediction ($Z_1=-0.81$), the observed isovector $M4$ cross section is only about half as large as anticipated. Since levels of $d_{5/2}$ character tend to have calculated energies that are about 1 MeV too low, the isoscalar $M4$ strength is probably best identified with the second predicted $T=0$, 4^- state at 18.43 which has an expected transition amplitude of $Z_0=-0.65$. However, as previously noted, the mixing of this level with the third $T=0$, 4^- state predicted at 19.58 MeV ($Z_0=0.36$) is sensitive to the assumed effective interaction.

D. Residual strength in the 19.5 MeV complex and the nature of the 18.2 MeV peak

On the right-hand side of Fig. 6 are shown the residual cross sections remaining after subtraction of the underlying continuum, 20.6 MeV resonance, and $M4$ line shape. For the purpose of illustrating the model dependence of the analysis, two residual cross sections have been calculated. The first, indicated by the plain error bars, corresponds to the continuous curves on the left-hand side of the figure which assume that the ^{12}C $M4$ form factor has the same q dependence as that observed in ^{13}C. The second, derived from the dashed curves and indicated by the circles, is based on the harmonic oscillator $M4$ fit to the high-q ^{12}C data alone. At $q_{\rm eff}=1.436$ fm^{-1}, the residual strength is seen to be broadly distributed, peaking in the vicinity of 19.6 MeV. However, for $q_{\rm eff}=0.498$ fm^{-1}, the lowest momentum transfer, the residual cross section concentrates more tightly near 19.35 MeV. Figure 5(b) shows the form factor for the residual strength between 18.7 and 20.3 MeV. As indicated by this figure, the model dependence of the $M4$ subtraction introduces little uncertainty up to $q=1.5$ fm^{-1}; however, beyond this point the residual form factor rapidly becomes ill defined. Nevertheless, the data that remain still do not follow the simple diffraction pattern expected from one dominant transition, but rather suggest the superimposed patterns of two or more competing transitions.

The simplest interpretation would therefore be that the residual cross sections consist of two components, a broad component which is preferentially excited in the region $q=1$–1.5 fm^{-1} and lies almost degenerate with the assumed isovector $M4$ peak at 19.6 MeV, and another peak centered near 19.35 MeV which prevails at lower momentum transfers. Any attempt to remove the higher-q com-

ponent by increasing the $M4$ subtraction results in negative residual cross sections for $q>2$ fm^{-1}.

The 19.35 MeV feature has been observed in numerous prior inelastic scattering measurements. Although its low-q character is broadly consistent with either a dipole or quadrupole assignment, two factors support an $M2$ identification. Firstly, there is an analog 2^- level near the corresponding excitation energy in ^{12}B, and secondly, theoretical studies have predicted appreciable strength for such a transition, as is observed. In the present calculations the relevant $T=1$, 2^- state lies at 18.34 MeV. A comparison of the observed and theoretical form factors is shown in Fig. 5(b). As has been seen for other magnetic form factors, with the exception of the first $\Delta T=1$, $M1$ transition, the predicted form factor is much too large. In order to obtain quantitative agreement with the data, the calculation must be multiplied by a factor of about 0.26.

Forward-angle, inelastic pion scattering measurements[14,16] indicate that the 19.35 MeV peak is strongly isospin mixed with a state observed at 18.32 MeV. This lower energy state has also been seen in (p,p') studies,[26,60] where the measured excitation energy is 18.30±0.03 MeV. Although there exists a slight discrepancy in the measured excitation energies, a possible counterpart to this level appears at 18.20±0.05 MeV in the (e,e') spectra shown in Fig. 2. The experimental properties of this (e,e') peak, 0.3±0.1 MeV wide at half-maximum, are slightly obscured since it abuts onto other broad resonance structures. Nevertheless, the results shown in Fig. 8 indicate that the form factor diffraction maximum occurs near $q=1$ fm^{-1}. Above 1.3 fm^{-1}, only upper limits can be deduced.

Current energy-level tables[12] suggest several alternatives to a $J=2^-$, predominantly $T=0$ assignment. For example, (p,γ) measurements[12] have indicated the existence of a possible 1^+, $T=0$ state at 18.13 MeV. However, not only is the observed 0.6±0.1 MeV width incompatible with the present results, but the (e,e') form factor calculated for the likely theoretical counterpart to this level also underestimates the data by a factor of 50. Although candidates have been found[12] for 3^- and 4^- states near 18.4 MeV, such states would be expected to have form factors which peak near $q=1.7$ fm^{-1}, not at 1 fm^{-1}. Finally, on the basis of qualitative agreement with calculated $E1$ form factors, Donnelly[10] and Yamaguchi *et al.*[24] suggested that the peak observed in (e,e') might have $T=1$, $J^\pi=1^-$. On the other hand, although analogs for nearby ^{12}C 1^- states exist in the low-energy spectrum of ^{12}B, no analog has yet been found for an 18.2 MeV, 1^- level. Thus the experimental properties of this level cannot be readily reconciled with any of the proposed alternatives to a $J^\pi=2^-$ assignment. At the same time, the low-q character of the 18.2 MeV peak in the (e,e') data can do no better than indicate likely excitation by means of a dipole or quadrupole operator.

As indicated in Fig. 1, a possible theoretical counterpart for a 2^-, predominantly $T=0$ state exists at an unperturbed energy of 17.68 MeV. However, the calculations show only weak isoscalar strength for this excitation, and are therefore inconsistent with measured (π,π') and (p,p') spectra where the peak is prominently seen.[16,60] Instead,

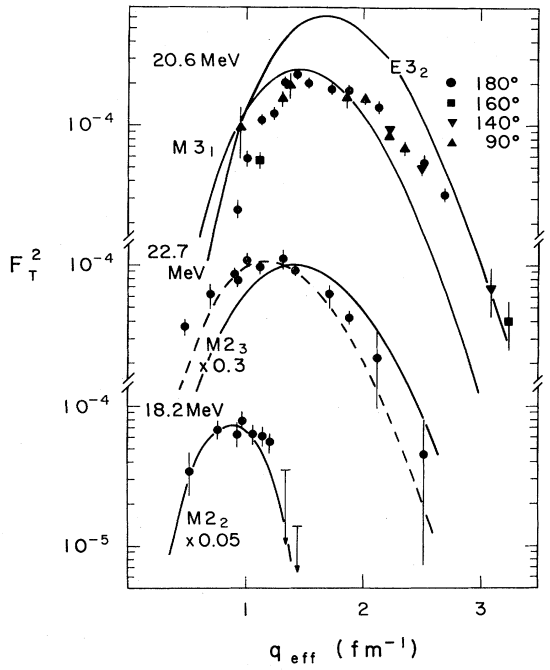

FIG. 8. Experimental data for the 20.6, 22.7, and 18.2 MeV transitions, and comparison with theoretical form factors calculated using $b=1.65$ fm. The theory for the transition to the 2_3^-, $T=1$ state displays some sensitivity to the shell-model assumptions, as indicated by the dashed curve, obtained with slight modifications to the effective interaction and single-particle energies. Note that the 18.2 MeV form factor is compared to the q dependence calculated for the transition to the 2_2^-, $T=1$ state.

the cross sections and angular distributions of the (π,π') and (p,p') data[60,61] are in much better agreement with the shell-model predictions for the second $T=0$, 2^- state, calculated to lie at 16.14 MeV. Moreover, the observed $l=2$ stripping strength, $S(d_{5/2})=0.85$ is consistent with that predicted for the 2_2^-, $T=0$ level, $S(d_{5/2})=0.70$. Thus, the 18.2 MeV peak is identified with the second $T=0$, 2^- level which is found about 2 MeV above the predicted excitation energy. A similarity may be noted with ^{16}O, where the shell model also underestimates the splitting of the lowest $T=0$, 2^- states.[37]

In the limit where the isoscalar contribution is ignored although, the extent of the isospin mixing between the 18.2 and 19.35 MeV states may be trivially estimated from (e,e') alone. Under this assumption, the ratio of the 18.2 and 19.35 MeV form factors will equal $\beta^2/(1-\beta^2)$, so that the observed 1:6 ratio near $q=1$ fm^{-1} gives $|\beta|=0.38$. The neglect of the $\Delta T=0$ cross section is, however, questionable in this case. Even though (e,e') is inherently less sensitive to isoscalar transitions, such large $\Delta T=0$ strength as has been observed in the (π,π') and (p,p') reactions can be expected to affect significantly the (e,e') cross section for the 18.2 MeV excitation. Due consideration of this isoscalar contribution could lower appreciably the previously estimated isospin mixing parameter. Further information on this mixing could, of course, be derived from a quantitative analysis of ($\pi^+,\pi^{+'}$) and ($\pi^-,\pi^{-'}$) results.

Returning to the residual 19.5 MeV form factor depicted in Fig. 5(b), it appears unlikely that the $M2$ component can account for much of the strength remaining in the vicinity of $q=1.3$ fm^{-1}. Some contribution to this excess strength can be expected to come from the broad analog of the $T=1$, 1^- level identified at 4.30 MeV in ^{12}B. According to the shell model predictions shown in Fig. 5(b), the $E1$ form factor is expected to make its main contribution above $q=1.5$ fm^{-1}; at lower momentum transfers it should exert little influence. Thus we are led to seek another origin for the strength observed near $q=1.3$ fm^{-1} in the residual cross section.

One possibility might be provided by the 1^+ level seen at 19.71 MeV in low-energy proton reactions.[12] It is not unreasonable to identify this level with the second $T=1$, 1^+ state found at 19.88 MeV in the (8—16)2BME Cohen-Kurath calculation.[9] Although this state is expected to have little transition strength at small q, corresponding to $B(M1)\uparrow=0.0528\ \mu_N^2$, a sizable $M1$ form factor is predicted near $q=1.3$ fm^{-1}. Unfortunately, the calculation still lies below the data by a factor of 3. A second alternative exists in a possible broad 2^+ state observed[12] at 19.40 MeV. Although the shell model gives the desired q dependence for $E2$ transitions to this region, the most strongly excited 2^+ state has a form factor which is too small by a factor of 7.

Thus the shell model seems pressed to account for the relatively large strength remaining in the $q=1.3$ fm^{-1} region after the subtraction of the assumed $M4$ component. This is somewhat disturbing since, as has been seen, the shell model almost invariably tends to overpredict the observed transverse cross sections.

E. The 20.6 MeV resonance

Figure 8 shows the form factor deduced for the 20.56 ± 0.05 MeV resonance which appears in the (e,e′) spectra with a natural width of 0.30 ± 0.05 MeV. This form factor peaks at a slightly lower momentum transfer than the $M4$ form factor, and, from a comparison of measurements made at different scattering angles, appears to be dominantly transverse in nature. In the vicinity of $q=1.5$ fm^{-1}, any corresponding longitudinal form factor must be less than 3×10^{-5}. Energy-level tables[12] currently indicate two states in this excitation region, one at 20.5 ± 0.1 MeV, and the other at 20.6 ± 0.1 MeV. The 20.5 MeV level is thought to have $J^\pi=3^+$, $T=1$, and the 20.6 MeV level is tentatively assigned $J^\pi=3^-$, $T=1$. These two levels find ready counterparts in the shell model spectrum, at calculated energies of 19.66 and 19.74 MeV, respectively. As Fig. 8 indicates, both the 3^- and 3^+ levels can be expected to make large contributions to the 20.6 MeV peak. The $E3$ and $M3$ form factors are reasonably consistent with the data, although the $M3$ q dependence could be improved by reducing the oscillator parameter b closer to the value suggested by the data on the $M4$ transition. In both cases the calculated magnitudes are too large, the $E3$ by a factor of 3, and the $M3$ by greater than 25%. In addition, the electric transition has an associated longitudinal $C3$ form factor which, according to the shell model predictions, should peak near $q=1.5$ fm^{-1} with a magnitude of 1.3×10^{-4}. Although this is at least a factor of 4 larger than the experimental result, it gives little guidance to the reduction that may be expected for the transverse $E3$ form factor. For the only resolved $\Delta T=1$ electric transition to the 16.11 MeV 2^+ state, the CK predictions exceed the measured $C2$ and $E2$ form factors by factors of 4 and 1.5, respectively.[62]

F. Evidence for a 2^-, $T=1$ state at 22.7 MeV

The final candidate for a magnetic transition is the 22.7 ± 0.1 MeV peak in the spectra shown in Fig. 2. This peak has a natural width of 0.45 ± 0.10 MeV, and neighbors a 22.0 MeV resonance which has a low-q character typical of an energetic $E1$ transition.[10,11] As shown in Fig. 8, the q dependence of the 22.7 MeV peak is reasonably consistent with that predicted for the transition to the 2_3^-, $T=1$ state, calculated to lie at 20.35 MeV. In common with the lower-energy $M2$ transitions, the predicted (e,e′) form factor is again too large and must be reduced by about a factor of 3 in order to fit the data. Previous suggestions of a strongly excited $T=1$, 2^- state near this excitation energy have been made on the basis of radiative pion capture measurements.[31]

V. CONCLUDING DISCUSSION

The main results of this work are summarized in Table IV. In most cases, the shell model predicts to within 1 or 2 MeV the excitation energies of observed magnetic transitions. Moreover, the measured q dependences are reasonably described, so that the model does provide useful guidance for the interpretation of the data.

What is remarkable is that the shell model's successes seem to exist despite its failure to correctly predict the magnitudes of the magnetic form factors: The calculations often exceed the data by factors of 2 or more. Thus, even though serious omissions from the shell model wave functions are indicated, the form factor shapes are reliably given. This situation is reminiscent of the comparison of theory and experiment for the longitudinal form factors of electric transitions. In this case the theory is usually a factor of 2—4 too small, but again the q dependences are well described. The enhancement of longitudinal form factors is credited to isoscalar core polarization effects.[63] The influence of polarization effects on magnetic transitions is more poorly understood. As discussed in Sec. II, magnetic transitions are generally mediated by two distinct terms, one involving the intrinsic magnetization of individual nucleons, and the other orbital convection currents. Whereas the intrinsic magnetization components dominate in isovector excitations, for isoscalar transitions the purely convective terms are often the more important. Both these contributions appear to be reduced relative to the shell model predictions. Ample evidence for the systematic quenching of isovector form factors may be seen in Table IV. Excluding excitations to the isospin-mixed, predominantly $T=0$ levels, the only form factor not predicted too large is for the 15.11 MeV, $M1$ transition in the range $q<1.5$ fm^{-1}. Moreover, Fig. 3 shows that the convection-current-dominated 11.83 MeV form factor is a factor of 6 smaller than calculated.

To investigate the effects of core polarization in the

TABLE IV. Summary of results. Except for the 15.11 and 19.59 MeV transitions, the ratio of the experimental and shell model cross sections, given in the rightmost column, does not include allowance for meson exchange contributions. In all cases, the ratios were based on comparisons at momentum transfers where the form factors attained their maximum values. Comparisons are made to both harmonic oscillator and Woods-Saxon theoretical predictions.

	E_x (MeV)		Γ_{Expt}	$\sigma_{\text{Expt}}/\sigma_{\text{Theory}}$	
$J^\pi;T$	Experiment	Theory	(MeV)	HO	WS
$1^+;0$	12.71	12.42		a	a
$1^+;1$	15.11	15.23		1.00	1.00
$2^-;0$	11.83	13.00		0.18	0.19
$2^-;1$	16.58	16.58		0.65	0.85
$(2^-;0)$	18.20±0.05	16.14	0.3 ±0.1	a	a
$2^-;1$	19.35±0.10	18.34	0.4 ±0.1	0.26[b]	0.27[b]
$(2^-;1)$	22.70±0.10	20.35	0.45±0.10	0.30	0.32
$3^+;1$	20.56±0.05	19.66	0.30±0.05	<0.75	<0.70
$4^-;1$	19.59±0.04	18.35	0.55±0.07	0.43[c]	0.51[c]

[a]Result strongly influenced by isospin mixing.

[b]Inclusion of isovector strength mixed into the 18.2 MeV peak increases the tabulated results by a factor of 1.2.

[c]The isospin-mixed 4^- states are analyzed as a doublet, utilizing (π,π') data from Ref. 25. See the text for details.

shell model would require very large bases, even to extend by $2\hbar\omega$ the bases used in our calculation. Nevertheless, restricted-basis $0\hbar\omega$ and $2\hbar\omega$ calculations show that 2p-2h correlations in the ground state of ^{12}C give rise to transition amplitudes which interfere destructively with the main $p \rightarrow sd$ amplitudes for the magnetic excitations discussed in this paper. (For the lowest-energy $E2$ and $E3$ transitions the interference is constructive, as expected.) Whether such correlations, when introduced into both the initial and final state wave functions, can account quantitatively for the observed quenching of magnetic transitions is an open question.

The experimental determination of isospin mixing matrix elements has been discussed. In particular, it was demonstrated that structure effects have the capacity to sensitively influence quantitative evaluations of isospin mixing based solely on (π,π') cross section ratios. The consideration of additional data from other reactions, such as (e,e'), (p,p'), and (p,n), can not only help to minimize these uncertainties, but also to supply information on the underlying pure $\Delta T=0$ and $\Delta T=1$ matrix elements. For theoretical calculations of charge-dependent isospin-mixing matrix elements, such information provides more direct checks than does data on the observed, mixed transition densities.

It has been proposed that delta isobar-nucleon hole configurations[3] may play an important role in the quenching of isovector magnetic transition strength.[7,64] This mechanism is expected to be more effective for low multipole transitions in high-Z nuclei. Thus little quenching is anticipated in a nucleus as light as ^{12}C, which may therefore be regarded as a useful null-effect case. The failure of the shell model to correctly predict the magnetic transition strengths, even in this relatively favorable instance, suggests that there still remains much to be learned about the more conventional model descriptions of magnetic form factors.

ACKNOWLEDGMENTS

The authors are indebted to Mr. M. A. Plum, Mr. B. Parker, Dr. A. Hotta, and Dr. R. C. York for assistance with the data taking, and to Dr. J. Dubach for valuable communications. Support for this work was provided by the U.S. Department of Energy under contracts with the University of Massachusetts and Bates Linear Accelerator Laboratory.

*Present address: Bates Linear Accelerator, Middleton, MA 01949.

[1]C. D. Goodman, C. A. Goulding, M. B. Greenfield, J. Rapaport, D. E. Bainum, C. C. Foster, W. G. Love, and F. Petrovich, Phys. Rev. Lett. **44**, 1755 (1980).

[2]R. S. Hicks, J. Dubach, R. A. Lindgren, B. Parker, and G. A. Peterson, Phys. Rev. C **26**, 339 (1982).

[3]A. Bohr and B. R. Mottelson, Phys. Lett. **100B**, 10 (1981).

[4]J. Delorme, A. Figureau, and P. Guichon, Phys. Lett. **99B**, 187 (1981).

[5]H. Toki and W. Weise, Phys. Lett. **92B**, 265 (1980).

[6]T. Suzuki, H. Hyuga, A. Arima, and K. Yazaki, Nucl. Phys. **A358**, 421 (1981).

[7]Toru Suzuki, S. Krewald, and J. Speth, Phys. Lett. **107B**, 9 (1981).

[8]N. Vinh-Mau and G. E. Brown, Nucl. Phys. **29**, 89 (1962).

[9]S. Cohen and D. Kurath, Nucl. Phys. **73**, 1 (1965).

[10]T. W. Donnelly, Phys. Rev. C **1**, 833 (1970).

[11]P. Antony-Spies, Nucl. Phys. **A188**, 641 (1972).

[12]F. Ajzenberg-Selove and C. Langell Busch, Nucl. Phys. **A336**, 1 (1980).

[13]C. L. Morris, J. Piffaretti, H. A. Thiessen, W. B. Cottingame,

W. J. Braithwaite, R. J. Joseph, I. B. Moore, D. B. Holtkamp, C. J. Harvey, S. J. Greene, C. F. Moore, R. L. Boudrie, and R. J. Peterson, Phys. Lett. **86B**, 31 (1979).

[14]C. L. Morris, Los Alamos National Laboratory Report LA-8303-C, 1980, p. 57.

[15]C. L. Morris, R. L. Boudrie, J. Piffaretti, W. B. Cottingame, W. J. Braithwaite, S. J. Greene, C. J. Harvey, D. B. Holtkamp, C. F. Moore, and S. J. Seestrom-Morris, Phys. Lett. **99B**, 387 (1981).

[16]C. F. Moore, C. J. Harvey, C. L. Morris, W. B. Cottingame, S. J. Greene, D. B. Holtkamp, and H. T. Fortune, Phys. Rev. C **26**, 2561 (1982).

[17]R. A. Lindgren, W. J. Gerace, A. D. Bacher, W. G. Love, and F. Petrovich, Phys. Rev. Lett. **42**, 1524 (1979).

[18]F. Petrovich and W. G. Love, Nucl. Phys. **A354**, 499 (1981).

[19]M. A. Plum, R. A. Lindgren, J. Dubach, R. S. Hicks, R. L. Huffman, B. Parker, G. A. Peterson, J. Alster, J. Lichtenstadt, M. A. Moinester, and H. Baer, Phys. Lett. **137B**, 15 (1984).

[20]J. Goldemberg and W. C. Barber, Phys. Rev. **134**, B936 (1964).

[21]G. A. Beer, T. E. Drake, R. M. Hutcheon, V. W. Stobie, and H. S. Caplan, Nuovo Cimento, Series 10, **53B**, 7 (1968).

[22]G. A. Proca and D. B. Isabelle, Nucl. Phys. **A109**, 177 (1968).

[23]J. W. Lightbody, Ph.D. thesis, University of Maryland, 1970 (unpublished).

[24]A. Yamaguchi, T. Terasawa, K. Nakahara, and Y. Torizuka, Phys. Rev. C **3**, 1750 (1971).

[25]C. F. Moore, W. B. Cottingame, K. G. Boyer, L. E. Smith, C. J. Harvey, C. L. Morris, H. A. Thiessen, J. F. Amann, M. Devereaux, G. Blanpied, G. Burleson, A. W. Obst, S. Iverson, K. K. Seth, R. L. Boudrie, and R. J. Peterson, Phys. Lett. **80B**, 38 (1978).

[26]J. M. Moss, C. Glashausser, F. T. Baker, R. L. Boudrie, W. D. Cornelius, N. Hintz, G. W. Hoffman, G. Kyle, W. G. Love, A. Scott, and H. A. Thiessen, Phys. Rev. Lett. **44**, 1189 (1980).

[27]J. R. Comfort, R. E. Segel, G. L. Moake, D. W. Miller, and W. G. Love, Phys. Rev. C **23**, 1858 (1981).

[28]C. A. Goulding, M. B. Greenfield, C. C. Foster, T. E. Ward, J. Rapaport, D. E. Bainum, and C. D. Goodman, Nucl. Phys. **A331**, 29 (1979).

[29]F. P. Brady and G. A. Needham, in *The (p,n) Reaction and the Nucleon-Nucleon Force,* edited by C. D. Goodman *et al.* (Plenum, New York, 1980), p. 357.

[30]K. Min, E. J. Winhold, K. Shoda, H. Tsubota, H. Ohashi, and M. Yamazaki, Phys. Rev. Lett. **44**, 1384 (1980).

[31]J. C. Alder, W. Dahme, B. Gabioud, C. Joseph, J. F. Loude, N. Morel, H. Panke, A. Perrenoud, J. P. Perroud, D. Renker, G. Strassner, M. T. Tran, P. Truol, and E. Winkelmann, in *Photopion Nuclear Physics,* edited by P. Stoler (Plenum, New York, 1978), p. 101.

[32]M. A. Kovash, S. L. Blatt, R. N. Boyd, T. R. Donoghue, H. J. Hausman, and A. D. Bacher, Phys. Rev. Lett **42**, 700 (1979).

[33]M. C. Wright, N. R. Roberson, H. R. Weller, D. R. Tilley, and Dean Halderson, Phys. Rev. C **25**, 2823 (1982).

[34]I. Sick, E. B. Hughes, T. W. Donnelly, J. D. Walecka, and G. E. Walker, Phys. Rev. Lett. **23**, 1117 (1969).

[35]R. S. Hicks and G. A. Peterson, *Proceedings of the International Conference on Spin Excitations in Nuclei* edited by F. Petrovich (Plenum, New York, in press).

[36]D. R. Inglis, Rev. Mod. Phys. **25**, 390 (1953).

[37]D. J. Millener and D. Kurath, Nucl. Phys. **A255**, 315 (1975).

[38]D. J. Millener, D. E. Alburger, E. K. Warburton, and D. H. Wilkinson, Phys. Rev. C **26**, 1167 (1982).

[39]J. A. Carr, F. Petrovich, D. Halderson, D. B. Holtkamp, and W. B. Cottingame, Phys. Rev. C **27**, 1636 (1983).

[40]W. Bertozzi, M. V. Hynes, C. P. Sargent, W. Turchinetz, and C. F. Williamson, Nucl. Instrum. Methods **162**, 211 (1979).

[41]G. A. Peterson, J. B. Flanz, D. V. Webb, H. deVries, and C. F. Williamson, Nucl. Instrum. Methods **160**, 375 (1979).

[42]I. Sick and J. S. McCarthy, Nucl. Phys **A150**, 631 (1970).

[43]F. Borkowski, P. Peuser, G. G. Simon, V. H. Walther, and R. D. Wendling, Nucl. Phys. **A222**, 269 (1974).

[44]R. S. Hicks, A. Hotta, J. B. Flanz, and H. deVries, Phys. Rev. C **21**, 2177 (1980).

[45]D. G. Ravenhall and D. R. Yennie, Proc. Phys. Soc. London **A70**, 857 (1957).

[46]See AIP document No. PAPS PRVCS 30-1-7 for 7 pages of tabulated cross section measurements. Order by PAPS number and journal reference from American Institute of Physics, Physics Auxiliary Publication Service, 335 East 45th Street, New York, NY, 10017. The price is $1.50 for microfiche or $5.00 for photocopies. Airmail additional. Make checks payable to the American Institute of Physics.

[47]J. B. Flanz, R. S. Hicks, R. A. Lindgren, G. A. Peterson, J. Dubach, and W. C. Haxton, Phys. Rev. Lett. **43**, 1922 (1979).

[48]P. A. M. Guichon and C. Samour, Nucl. Phys. **A382**, 461 (1982).

[49]N. C. Mukhopadhyay and J. Martorell, Nucl. Phys. **A296**, 461 (1978).

[50]J. Dubach and W. C. Haxton, Phys. Rev. Lett. **41**, 1453 (1978).

[51]C. L. Morris, W. B. Cottingame, S. J. Greene, C. J. Harvey, C. F. Moore, D. B. Holtkamp, S. J. Seestrom-Morris, and H. T. Fortune, Phys. Lett. **108B**, 172 (1982).

[52]J. Delorme, M. Ericson, A. Figureau, and N. Giraud, Phys. Lett. **89B**, 327 (1980).

[53]M. Haji-Saeid, C. Glashausser, G. Igo, W. Cornelius, M. Gazzaly, F. Irom, J. McClelland, J. M. Moss, G. Pauletta, H. A. Thiessen, and C. A. Whitten, Jr., Phys. Rev. Lett. **45**, 880 (1980).

[54]R. S. Hicks, R. A. Lindgren, B. Parker, G. A. Peterson, H. Thiessen, H. Crannell, and D. Sober, Los Alamos National Laboratory Report LA-8303-C, 1980, p. 292.

[55]W. deJager, H. deVries, and C. deVries, At. Data Nucl. Data Tables **14**, 479 (1974).

[56]R. S. Hicks (unpublished).

[57]T. W. Donnelly and W. C. Haxton, At. Data Nucl. Data Tables **23**, 103 (1979).

[58]F. Petrovich, R. H. Howell, C. H. Poppe, S. M. Austin, and G. M. Crawley, Nucl. Phys. **A383**, 355 (1982).

[59]D. Halderson, R. J. Philpott, J. A. Carr, and F. Petrovich, Phys. Rev. C **24**, 1095 (1981).

[60]K. W. Jones, C. Glashausser, S. Nanda, R. de Swiniarski, T. A. Carey, W. Cornelius, J. M. Moss, J. B. McClelland, S. J. Seestrom-Morris, J. R. Comfort, J. L. Escudie, M. Gazzaly, N. Hintz, G. Igo, M. Haji-Saeid, and C. A. Whitten, Phys. Lett. **128B**, 281 (1983).

[61]T.-S. H. Lee, D. Kurath, and D. J. Millener (unpublished).

[62]J. B. Flanz, R. S. Hicks, R. A. Lindgren, G. A. Peterson, A. Hotta, B. Parker, and R. C. York, Phys. Rev. Lett. **41**, 1642 (1978).

[63]P. J. Ryan, R. S. Hicks, A. Hotta, J. Dubach, G. A. Peterson, and D. V. Webb, Phys. Rev. C **27**, 2515 (1983).

[64]F. Osterfeld, S. Krewald, J. Speth, and Toru Suzuki, Phys. Rev. Lett. **49**, 11 (1982).